International Journal of Mass Spectrometry 280 (2009) 57–64

Contents lists available at ScienceDirect

International Journal of Mass Spectrometry

journal homepage: www.elsevier.com/locate/ijms

A quantum modeling of the chemistry of LiH^+ with He from *ab initio* calculations: Ionic reactions in He nanodroplets

M. Wernli, E. Scifoni [1], E. Bodo, F.A. Gianturco *

Department of Chemistry and CNISM, University of Rome "la Sapienza", Ple A. Moro 5, 00185 Rome, Italy

ARTICLE INFO

Article history:
Received 23 May 2008
Received in revised form 9 July 2008
Accepted 18 July 2008
Available online 30 July 2008

This work is dedicated to Professor Zdenek Herman, a creative experimentalist, a prolific scientist and a sensitive artist, on the occasion of his 75th birthday, with our best wishes to a good friend.

Keywords:
Helium droplets
Potential energy surfaces
Quantum chemistry calculations
Reactive minimum energy paths

ABSTRACT

The fully three-dimensional ground and first electronically excited states of the $[LiHHe]^+$ system were computed with *ab initio* methods, using a self-consistent field treatment followed by a multi-reference configuration interaction calculation. The topology and reactive pathways of the surfaces are analysed at different configurations extending the understanding of the possible dynamics on these surfaces with respect to previous studies limited to lower dimensionality. The behavior of LiH^+ inside or at the surface of a helium droplet is surmised from our findings, along with some suggestions on possible ways with which the different reactive and deexcitation phenomena occurring in this environment could be experimentally detected.

1. Introduction

The study of lithium hydride chemistry in reaction with the lightest atoms (hydrogen and helium) is of importance in several fields, one of which being the understanding of elementary chemical processes occurring in the early universe [1]. The complex chemistry is supposed to have initiated with the appearance of the first dihydrogen (H_2) molecules, during the recombination epoch ($\sim$ 1000 years after the big bang), when neutral and ionic lithium hydrides could both be involved in the formation of the first H_2 molecule. To fully understand this process of formation, one has to know also the efficiency of rival processes at play in the same environment. The helium atom is the second most abundant species after hydrogen; it is hence of importance to know the specific behavior of lithium hydrides with this atomic partner and the details of their chemical interactions.

A second field of interest for the present system is provided by the study of the helium nanodroplets. Recent experimental progresses has allowed researchers, by combinations of older and well known techniques like matrix isolation in crystals and supersonic molecular beams, to have access to the controlled formation of liquid ^4He nanodroplets with sizes ranging from 10^2 to 10^8 atoms, which provide in turn a unique, cold environment (at $T \leq 0.37$ K) for the study of physico-chemical processes involving embedded species [2–4].

An extensive amount of theoretical work has now shown that all closed-shell atoms or molecules, with the exception of the alkali and alkaline earth atoms [5], are heliophilic, i.e., are absorbed inside the helium droplets. For open-shell systems and ions, much less work has been published, and the question is still open for several of such systems as to whether they are completely heliophobic, i.e., remain at the surface of the droplet, or present instead a heliophilic behavior depending on the size of the droplet. In this case one therefore wishes to know if and how the solubility depends on the number of He atoms in the droplet.

Indeed, the presence of an ionic impurity inside the droplet has been shown to cause strong modifications of the local order of the droplet. Impurities as ionic alkali metals (see Ref. [6]) are expected to cause a local increase of helium density, due to electrostriction, to a point where some local order is achieved and it creates local near-solid structures, the so-called snowballs [7]. This model has been widely used to interpret experiments and it explains for

* Corresponding author.
E-mail address: fa.gianturco@caspur.it (F.A. Gianturco).
[1] Present address: Frankfurt Institute for Advanced Studies, Goethe University, Frankfurt am Main, Germany.

1387-3806/$ – see front matter © 2008 Elsevier B.V. All rights reserved.
doi:10.1016/j.ijms.2008.07.019

example why, at odd with neutral species, positive ions have a very low mobility in liquid He and in helium droplets [8].

The self-organisation and aggregation of dopants inside helium droplets created by the low temperature of this environment gives rise to the possibility of studying chemical reactions with strong orientational dependence, their trapping in global van der Waals minima or other favoured configurations possibly enhancing or creating reactive channels which would be unlikely to occur in other environments. As an example, several complexes of radicals either reactant or products can now be produced inside droplet and their structures analysed with high resolution spectroscopy [9].

There are two possible classes of reactions to study inside the droplets: dopant–dopant reactions, as mentioned above, and reactions of the dopant with its He environment. Experimental techniques used to initiate this type of reactions include photo- and electron-impact ionisation: an ionised He^+ is created (a "hole") and then it migrates because of induction forces [10] towards the embedded species, eventually ionising it. But one can also directly ionise the dopant species, passing from a non-reactive neutral dopant–droplet interaction to the reactive ionic dopant–droplet situation. This is the case on which the present work is focused.

To understand the dynamics of ionic dopants inside the droplet, it is thus very helpful to also study the different processes which are possibly at play: we could, in fact, surmise that after entering the droplet the rovibrationally excited LiH^+ dopant can either cool off by collisional internal energy transfer to the surrounding matrix (thereby provoking evaporation of helium atoms from the droplet) or the dopant can instead be able to react with one of the surrounding helium atoms to form $LiHe^+$, the different products depending on the nature of the interaction at play. It is this latter interaction which we wish to analyse in the present work.

Notwithstanding the large amount of theoretical and experimental work about dopants in droplets, very little is known about the forces at play at the microscopic level when chemical reactions become present and are energetically allowed. This is due in part to the sizable computational cost of a fully three-dimensional potential energy surface, a feature which still limits calculations to few-electron systems or otherwise to using crude approximations in order to reduce the dimensionality of the problem. Ref. [11], for example, showed that the many-body (MB) effects in a helium matrix are generally small and therefore the interaction potential of the dopant inside the droplet can be reasonably approximated by a sum of 2-body (2B) (dopant- ^{4}He) potentials. On the other hand, when chemical reactions are to be considered among the outgoing channels, the full effects of MB forces need to be included in any realistic estimate of the relevant potential energy surfaces.

Let us recall that the present system has been already considered in two of our previous work [12,13]. In both cases, though, the dimensionality of the system was reduced. In Ref. [12], we examined possible reactions on the first two electronic states of the system which reacts only along collinear configurations. For the ground state, we found a shallow stable ($\simeq 30\,cm^{-1}$) van der Waals configuration when He approaches the Li-side of the target and that the reaction forming Li^+He is endothermic, hence only likely to occur when the molecular ion is vibrationally excited. The first electronically excited state proved to be topologically different because of the different charge collocations in LiH^+ and therefore, the reaction could develop without barrier from LiH^+ to HeH^+ when the helium atom would approach the H-side of the target.

In Ref. [13], a nonreactive interaction between partners with the Li^+H bond length fixed at its ground state equilibrium distance ($r_e = 2.191$ Å), was used to study the clustering of helium atoms around the cationic dopant in a droplet environment. We found that up to 30 He atoms would locate in a cap-like structure surrounding the Li-side of the cation, while the H atom would remain outside this structure.

The present work is therefore an extension of our analysis to the first fully three-dimensional potential energy surface (PES) for the first two electronic states of this ionic system. The increased dimensionality will allow us to discuss the reliability of the simplifications used in our two previous studies by allowing us to assess the importance of nonlinear approaches to reactive channels, the influence of the electronic state of LiH^+ on the structuring of He atoms around it and the possible deexcitation (vibrational or electronic) of LiH^+, when reacting with its helium environment. While addressing these questions, we shall also try to suggest ways in which these phenomena could be experimentally detected in the droplets.

The paper is organised as follows: Section 2 gives the details of the *a* b initio computation and of the numerical fitting of the ground and first excited PESs; Section 3 analyses the ground state topology both in the collinear configurations and for the non-collinear arrangements. The first excited PES is described in Section 4, while Section 5 summarises our conclusions.

2. Details of calculations

If we define as r_1 the H–He distance, r_2 the Li–H distance and r_3 the Li–He distance, the three-dimensional interaction potential (i.e., after subtracting the individual atomic energies) can be expressed as

$$V_{tot}(r_1, r_2, r_3) = V_{2body} + V_{3body} + O(4body), \quad (1)$$

where $V_{2body} = \sum_k V_{2B}^{(k)}(r_k)$, $k = 1, 2, 3$ is the sum of the three diatomic potentials. It is generally accepted that contributions of more than 3body (3B) interactions could be considered as negligible. We hence have to compute accurate 2B potentials for all three possible pairs of atoms, H–He, Li–H and Li–He, with the 3B potential of similar accuracy. The strategy used by us furthermore relies on the fact that 2B potentials are the dominant contributions to V_{tot}. It therefore involves four basic steps:

1. *ab initio* computation and fitting of the 2B potentials;
2. *ab initio* computation of V_{tot} on a finite grid of geometries $\{g_i\}$, $i < N$;
3. build V_{3B}; i.e., compute $V_{3B}(g_i) = V_{tot}(g_i) - \sum_k V_{2B}^{(k)}(g_i), \forall i$. We see at this stage that it is important that the total and the diatomic potentials were calculated with the same *ab initio* strategy. We also need to fit $V_{3B}(g_i)$ to get a continuous 3B potential $V_{3B}(\omega)$, $\omega \in \mathbb{R}^{+3}$, with $\omega = (r_1, r_2, r_3)$ being the atom–atom coordinates;
4. build $V_{tot}(\omega) = \sum_k V_{2B}^{(k)}(r_k) + V_{3B}(\omega)$. At this stage, depending on whether or not we are able to find accurate potentials in the current literature, we may decide to add different (perhaps better) diatomic potentials than those computed in step 1.

All present *ab initio* calculations were performed using the GAMESS[14] program.

2.1. The raw points generation from ab initio methods

2.1.1. Diatomics

The three diatomic potentials are those already discussed in Ref. [12]. To the initial sets of geometries, we furthermore added a small number of points for the LiH potential at short-range in order to ensure a reliable extrapolation of the repulsive part of that potential. Let us now recall briefly the *ab initio* strategy employed: the radial grid for all three potentials consisted of a total of about 30 points each, with radial ranges of 0.3–10 Å for H–He, 1.5–9 Å for

Li–H and 0.8–5 Å for Li–He, respectively. For all these points the potential was calculated starting from an HF initial guess which provided the ensuing complete active space for the self-consistent field (CASSCF) calculations, whose optimised molecular orbitals served in turn as input for the final multi-reference configuration interaction (MRCI) computations. All parameters were optimised to ensure convergence of the electronic ground and first excited states of the diatomics. The active space used for all calculations contained nine orbitals. See Ref. [12] and references therein for more details on the atomic basis used.

2.1.2. 3B geometries

We have employed as many as possible the earlier 988 points for the collinear configurations: $[Li–H–He]^+$ and $[He–Li–H]^+$ already discussed by Ref. [12]. To this, a new set of 803 points was added to describe the nonlinear configurations. The strategy used to obtain them was twofold: (i) for each LiH distance on a grid ranging from 1.6 to 4.4 Å the potential was computed at six equidistant angles. Hence this was done for each grid distance of the He atom to the centre of mass of the Li–H target, ranging from 1.3 to 5.8 Å. At short distances, the angular grid was increased by three to six more points to account for the large anisotropy of the potential in such strong interacting regions. Each point was computed not starting from a new HF calculation, but using instead as an initial guess the SCF orbitals of the closest neighbouring point. These calculations will hereafter be referred to as angular scans; (ii) to avoid oscillations in the subsequent fitting that would have appeared because of the near-periodicity of the grid employed, we computed a smaller set of points in a randomly selected set of geometries lying in the same range as the angular scans. This new set of non-collinear geometries consisted in turn of 104 new points: the *ab initio* method used for these points was exactly the same as for the collinear configurations we used in Ref. [12]. The accuracy of all the points computed depends on the value of the potential itself, but we estimate it to be within $\sim 3\,cm^{-1}$ for $|V_{tot}| < 300\,cm^{-1}$ and around 1% for larger values of the total potential. In the end, the total number of points employed in the fitting which we describe below was of 1895 points for the lower and first excited PES.

2.2. The many-body fitting of the overall PES

2.2.1. Diatomics

The diatomic asymptotes associated with the ground state 3B surface are $Li^+ H(X^2\Sigma^+)$ and $Li^+He(X^1\Sigma^+)$. For the first electronically excited PES, they are $Li^+H(2^2\Sigma^+)$ and $HeH^+(X^1\Sigma^+)$ (see [12], Figs. 1 and 2).

All four asymptotic components, together with neutral "molecules" [HHe] and [LiHe], were fitted using our variant of the analytical form suggested by Aguado and Paniagua [15] for diatomics:

$$V_k(R_k) = \frac{c_0\, e^{-\alpha_k R_k}}{R_k} + \sum_{i=1}^{N} c_i \rho_k^i, \tag{2}$$

where

$$\rho_k = R_k\, e^{-\beta_k^{(l)} R_k}, \tag{3}$$

with $k = 1$ for HHe, 2 for LiHe and 3 for LiH and $l = 2$ for diatomics. The fit was weighted by using a function giving greater importance to the attractive range and low-energy repulsive points. The parameters and outcome of the fitting are summarised in Table 1. No equilibrium distance or minimum value are given for LiHe and HHe as these two diatomic partners are not bound, although their repulsive potentials also need to be globally fitted within the full reactive surfaces of the present study.

Table 1
Optimised fitting parameters and results for the first two electronic states of the three diatomics

	N	β	V_{min} (cm^{-1})	R_{min} (Å)
$Li^+H(X^2\Sigma^+)$	6	2.66	−1113.8	2.192
$LiH^+(A^2\Sigma^+)$	6	2.34	−3938.5	3.932
$Li^+He\ X^1\Sigma^+)$	3	4.1	−642.5	1.898
LiHe	7	3	–	–
HeH	7	4.6	–	–
$HeH^+(X^1\Sigma^+)$	11	8.3	−16444.8	0.7744

At short-range an exponential extrapolation was added so that in the end all diatomic potentials were obtained up to at least 50,000 cm^{-1} in their repulsive ranges. At long-range, a power-law extrapolation of the R^{-n} type was used with $n = 6$ for neutral systems and $n = 4$ for ionic ones, which are in both cases the respective leading terms in the multipolar expansions. On both sides, the connection between the many-body fitting with both the short- and long-range extrapolations was made to occur smoothly by the use of a doubly differentiable connecting function:

$$C(x) = \frac{1}{2}\left[1 - \cos\{(1 - \cos(\pi x))\frac{\pi}{2}\}\right], \tag{4}$$

where the connection between the extrapolating function $f(r)$ and the potential $g(r)$ in an interval $[r_a, r_b]$ is made at short-range via the formula:

$$\left[1 - C\left(\frac{r - r_a}{r_b - r_a}\right)\right] f(r) + C\left(\frac{r - r_a}{r_b - r_a}\right) g(r), \tag{5}$$

The left coefficient "turns off" $f(r)$, while the right one "turns on" $g(r)$. At long-range the roles of $f(r)$ and $g(r)$ are interchanged.

For all six diatomics involved the quality of the optimised fitting was excellent, with a standard deviation which was always $< 0.1\ cm^{-1}$. The fitting quality of the bound states was furthermore assessed by computing their vibrational eigenfunctions and eigenenergies via the LEVEL program [16]. For $Li^+H(X^2\Sigma^+)$, we found the same number of bound states (7) as encountered by Refs. [17,18], with differences of less than $4\,cm^{-1}$ for all states. For $Li^+H(A^2\Sigma^+)$, to the best of our knowledge, no bibliographic data exist and we obtained 25 bound states, the last 2 being less certain because of the smallness of their binding energies: 1.21 and $0.18\,cm^{-1}$ below dissociation, respectively. For Li^+He, again no data could be found in the literature: we got eight bound states, two of them being very weakly ($< 1\,cm^{-1}$) bound. Finally for HeH^+, we found 12 bound states, all in agreement (within $5\,cm^{-1}$) with the earlier data of Ref. [19].

2.2.2. 3B and total potential

Having fitted all diatomic states following accurately the *ab initio* points, we then carried out point (3) of the four-step procedure outlined before, i.e., compute on the grid of the total potential the purely 3B contributions. We may say about this procedure that it justifies our splitting strategy in the sense that the 3B potential was found nearly always to be much smaller that the total potential (except, of course, for regions where a rising repulsion wall increases above its onset). The electronic ground state was fitted using the form:

$$V_{3B}(r_1, r_2, r_3) = \sum_{i,j,k}^{M} d_{ijk} \rho_1^i \rho_2^j \rho_3^k, \tag{6}$$

as taken from Ref. [15]. The ρ follows the definition of Eq. (3), but with $l = 3$. We used an optimisation procedure to find the best three nonlinear β parameters and the order M of the fitting. With $\beta_{HHe} = 2.0$, $\beta_{Li^+He} = 1.2$, $\beta_{Li^+H} = 0.8$ and $M = 7$ (which

corresponds to 101 basis functions), using a V_{tot}^{-W} weighting, where the optimal weighting power was here found to be $W = 0.3$, we got a 0.9 cm^{-1} standard deviation for all our raw points. The long-range potential turned out to be nearly exclusively 2-body, and therefore no extrapolation of the pure 3B potential needed to be done: it was simply put to zero at long-range using the connecting function given in Eqs. (4) and (5).

Reassured by the good quality of our diatomic calculations, further assessed by a comparison of our vibrational levels with the available data, we completed the four-step procedure by constructing the total potential as a sum of 2B and 3B contributions. From the split-fit procedure used and the errors of the various fitting results, we can estimate the overall fitting quality to be within a few cm^{-1} for the well regions of the total potential and around 1–2% for values in the repulsive range above a few hundred cm^{-1}, a precision coherent with that provided by the *ab initio* calculations.

Finally, we obtained the electronic ground state of the $[LiHHe]^+$ system, with a typical 10 cm^{-1} reliability for potential values up to 500 cm^{-1} and 2–3% for V between 500 and 50,000 cm^{-1}. This is an acceptable precision with respect to the further uses of this PES for reactive scattering and for structural studies for which it was intended.

The first electronically excited PES for the present system was also retrieved from the same run of GAMESS[14] calculations, hence on the same grid of 1895 geometries. The 3B breakup limit of this state lies 0.3021 hartree (66,303 cm^{-1}) above that of the ground state. As mentioned before, the basis sets used were optimised in order to obtain both states with reliable convergence. Nonetheless, the excited state is expected to be less accurate, especially in the regions of strong repulsive interaction.

We used the same fitting strategy as for the ground state. Through nonlinear optimisation we obtained the following parameters for the 3B fitting: $M = 9$ (hence using 195 basis functions), $\beta_{HeH^+} = 1.8$, $\beta_{LiHe} = 0.9$ and $\beta_{LiH^+} = 1.2$. The fitting was weighted using $V_{tot}^{-0.6}$. Finally, with the converged parameters we obtained a 2.0 cm^{-1} standard deviation for the whole surface, a fitting precision which is even better than that achieved by the *ab initio* calculations for this state.

3. Surveying the lowest surface

In this section, we will analyse the outcomes of the global fitting of the ground-state PES. Figs. 1–4 show PES cuts and computed minimum energy paths (MEPs) for the He atom approaching the Li atom at different angles with respect to the LiH bond. On some MEP panels we have also reported the first five vibrational levels of the relevant diatomic asymptotes. All these figures show once again, by the absence of spurious oscillations, the rather good quality of the fitting of the *ab initio* calculations achieved in the present work.

Fig. 1 reports the PES and MEP for the He–Li–H collinear orientations: we can see on the upper panel that the surface is strongly reactive, since it goes exothermically from the Li^+He ion on the left side to the Li^+H cation on the right, thus indicating as more favourable the permanence of the Li^+H initial partner. Our fitting of the surface places the lower and upper asymptotes at −1113 and −643 cm^{-1}, respectively, with a minimum at −1736 cm^{-1}, which is also the global minimum of the whole surface: it occurs at $r(LiH) = 2.20$ Å and $r(LiHe) = 1.90$ Å.

We also see that the reaction barrier is here fairly small since the first vibrationally excited state of the Li^+H reagent partner is only slightly below the ground vibrational state of the Li^+He cationic product. It suggests that even at the lower collision energies the reactive channel can be already open for an initially excited Li^+H partner to He. Most probably, the proximity of the $v = 1$ state of

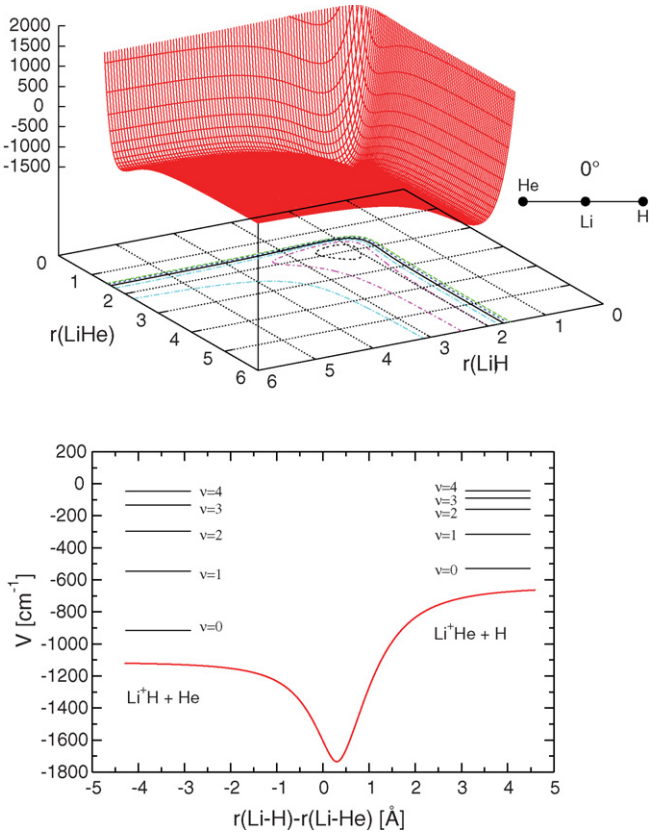

Fig. 1. Upper panel: Ground-state potential energy surface for He approaching Li^+H at 0°. Distances are in Å, potential values in cm^{-1} and the projection on the plane shows as a solid line the $V = 0$ profile. Lower panel: minimum energy path for the same orientation. The vibrational levels of the two diatoms are shown above the $v = 0$ reference energies.

Li^+H with the $v = 0$ state of Li^+He, as well as that of $v_{Li^+H} = 2$ with $v_{Li^+He} = 1$, and given the strength of the attractive well, could be the source of resonances in scattering processes, an indication that indirect reactive mechanisms are likely to play here a significant role.

Fig. 2 reports the PES at $\theta = 60°$ and 90°. From this figure, we see that the surface remains qualitatively unchanged whenever the He atom approaches the cation on its Li-side. This isotropy at the small angles is due to the fact that the electronic charge is essentially located on the lithium atom, so that the interaction potential is largely dominated by the isotropic charge–polarisability contributions. When still increasing the angle, however, the global minimum goes progressively (albeit slowly) to larger values, eventually reaching a point where there is no more a minimum energy configuration and the MEP moves directly from one asymptote to the other. This occurs between ∼ 120° and ∼ 140°. Fig. 3 illustrates this on the PES and MEP, at $\theta = 120°$. From this and larger angles of approach, the He atom first sees the repulsive H-side of the dimer. Hence the appearance of barrier, reflecting the fact that when He approaches Li^+H on the H-side, it first encounters a large repulsive wall due to the Pauli repulsion between the electron density on H and the two-electron density on the He atom.

The other collinear configuration, $[LiHHe]^+$ is presented in Fig. 4 (note that the coordinates have been changed for pictorial convenience). We see on the right side of the PES (upper panel) the nearly isolated Li^+H asymptote, while there is no bound HHe asymptote on the left, the interaction between the two atoms being purely repulsive. The MEP, on the lower panel, further shows that there exists a small van der Waals minimum when

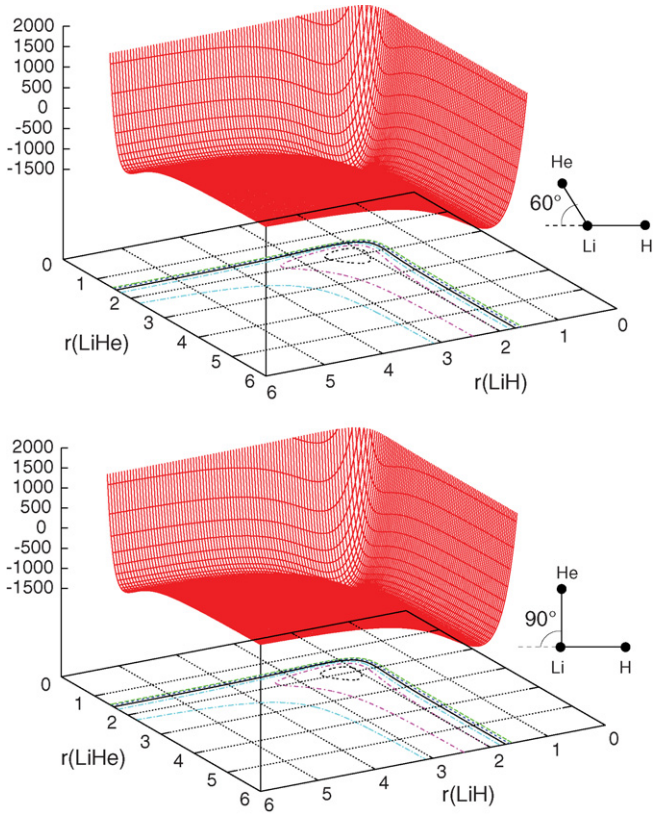

Fig. 2. Same as the upper panel of Fig. 1, for $\theta = 60^\circ$ (upper panel) and $\theta = 90^\circ$ (lower panel).

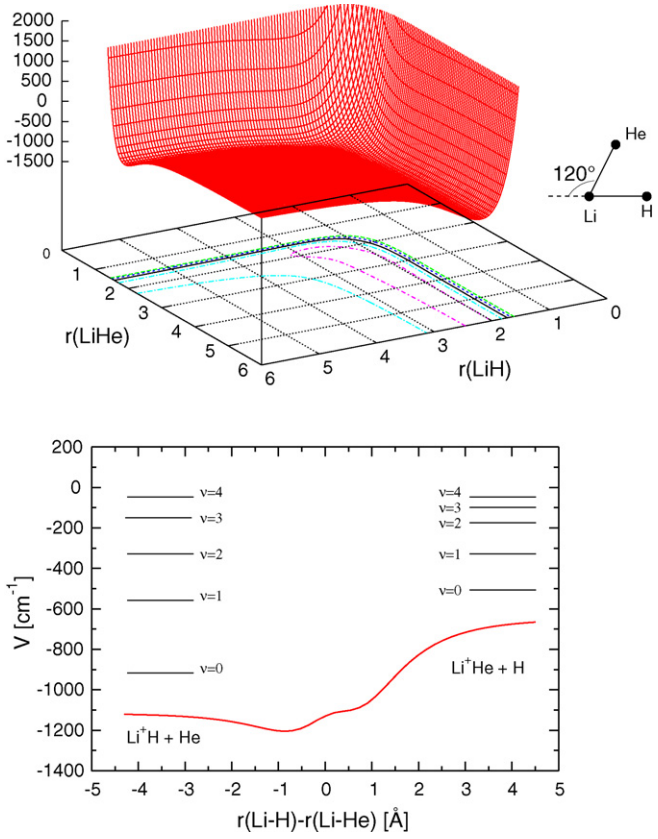

Fig. 3. Same as Fig. 1, at a $\theta = 120^\circ$ approaching angle.

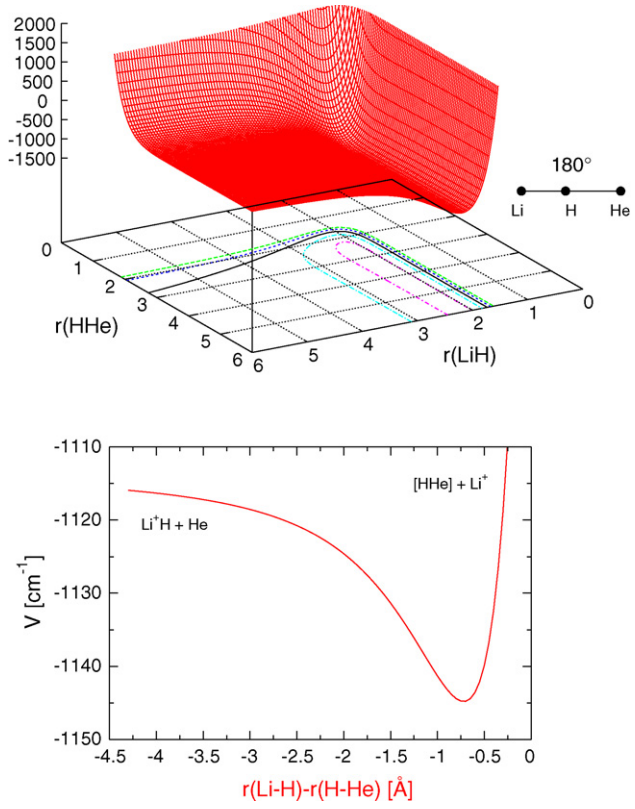

Fig. 4. Same as Figs. 1 and 3, at a $\theta = 180^\circ$ approaching angle.

$V_{tot} = -1145\ cm^{-1}$, which lies some $35\ cm^{-1}$ below the bound Li^+H asymptote. Thus, reaction is not likely to be possible when the helium atom is approaching the H-side of Li^+H around this collinear orientation.

In conclusion, the surface we have just surveyed presents a small interval of angular approaches for which no reaction will be possible, on the H-side of the LiH^+ cation. On the other side, whenever even a rather small amount of internal energy is present in the cation in the form of vibrational excitation, or if the kinetic energy content increases, the small endothermicity of the reaction should allow it to happen for an extended range of angular approaches of He towards the Li-side of the cation. Obviously, in real collisional processes, the He atom will not follow only one specific orientation; the classical picture is that it will find its way to the best accessible path, which means, however, that some of the possible trajectories will involve arrangements which, energetically at least, cannot lead to product formation at low collision energies. When considering the collisional process between a vibrationally excited Li^+H cation and He, the anisotropy on the PES will reflect itself in possibly yielding comparable probabilities for the vibrational deexcitation or for the exchange reaction evolving towards a less internally excited Li^+He product.

When addressing the problem of Li^+H interacting within a helium droplet, it could be useful to consider at least two possible situations: (i) a cationic diatom directly entering the droplet or (ii) a neutral LiH already trapped inside the droplet and subsequently ionised by electron or photon impact. As the second situation can involve electronic excitation of the cation, it will be discussed below, in the section about the first electronically excited PES (Section 4). Let us now consider the first case a bit further. We recall that calculations of Ref. [13] fixed the cation interatomic distance at its equilibrium value. Thus, neither its vibration nor the reactive exit channels could be taken into account in this purely

structural analysis of the problem, i.e., of the relative collocations of the He adatoms surrounding the doping cation.

Let us now consider first the nonreactive situations: even with the cation is in its ground vibrational state, the geometry which the closest helium atoms will "see" should be given by the larger, vibrationally averaged distance of the target molecule. If the cluster calculations were therefore to be repeated using a larger Li^+H geometry, one could expect larger snowball structures to be computationally observed, as discussed in Ref. [6].

If we further consider the Li^+H to enter the He droplet in an excited vibrational state, two possible events may occur: (i) a vibrational relaxation, i.e., the internal energy of the cation is transfered to the atoms of the droplet, this transfer causing rapid solvent atom evaporations up to several hundred He partners [20] or, (ii) the chemical reaction discussed before, i.e., the one forming Li^+He. We have seen that this may occur even at low relative velocities and already for Li^+H in its $v = 1$ level. In this case, the hydrogen atom would probably be ejected from the droplet after migration to its surface [21,22], while the behavior of the newly formed cation could vary from remaining on the surface of the droplet with the lithium inside it, to total solvation well inside the droplet, depending on its residual energy. To predict the preferential behavior would definitely require to have a PES for the $LiH^+(He)_n$ system which we could conceivably construct as a sum-of-potentials [6] for each selected vibrational state of the cation and using the one produced by the present study.

Experimentally, to see whether one process occurs or the other would require to collect the He signal for the ejected atoms, i.e., the number of He atoms as a function of time and compare what is found from the evaporation of He from the pure droplet with that due to the additional presence of the cation. In case one were to have only dissipation of the internal energy of the cation, the evaporative yield may then be larger than that of the reaction. Hence, one should possibly not observe a marked increase of the number of helium atoms that leave the droplet. The direct measurement of the He yield would almost certainly be a difficult task, especially so for small droplets. In the latter case, an easier way to see if the reaction occurred could then be through the use of a mass spectrometer; bare ions or positive ions surrounded by a small number of He adatoms are indeed more easily detected via mass spectra [23,24].

Finally, another way of testing whether the reaction has occurred or not is by using a laser source that would be scanning the frequencies around the vibrational frequency of one of the two cations. With this probing we could, at the same time, know if the reaction occurred by detecting one of the cations, and also have some insight as to whether a snowball has formed around it, a feature after equilibration which could modify its vibrational spectrum.

4. The next excited electronic surface

The present section discusses the main features of the first electronically excited state as provided by the fitting described in Section 2.2.2. Figs. 5 and 6 show the computed MEPs at four representative relative orientations. The zero of energy is given, as before, by the 3-atom breakup.

As mentioned in Section 2.2.1, the two asymptotic species of the reaction are LiH^+ on one side and HeH^+ on the other side, with a large exothermicity of 12506.3 cm^{-1}. Note that the angle convention chosen here for the plots defines the orientation from the H-side of the LiH partner, which is different from that we followed for the ground state. We see from the panels that in the Li–H–He collinear configuration (Fig. 5, upper panel), the reaction from LiH^+ to HeH^+ goes down without a barrier, but with a van der Waals minimum at −17, 730 cm^{-1} in the product valley. It is located about 1110 cm^{-1} below the HeH^+ diatomic asymptote, thus indicating the formation of a stable triatomic complex. When increasing the angle, the Li–He repulsion begins to play a significant role and this repulsion is reflected in the appearance of a "hump" at 60° (Fig. 5, lower panel), while the final minimum becomes even lower, due to 3B contributions. As we found for the case of the ground state dis-

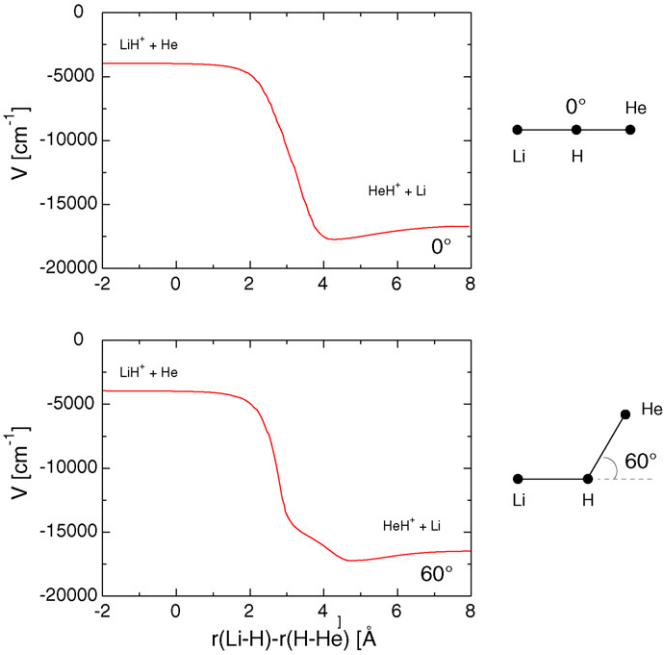

Fig. 5. Computed minimum energy paths for the first electronically excited state at different orientations. Upper panel: $\theta = 0$; lower panel: $\theta = 60°$.

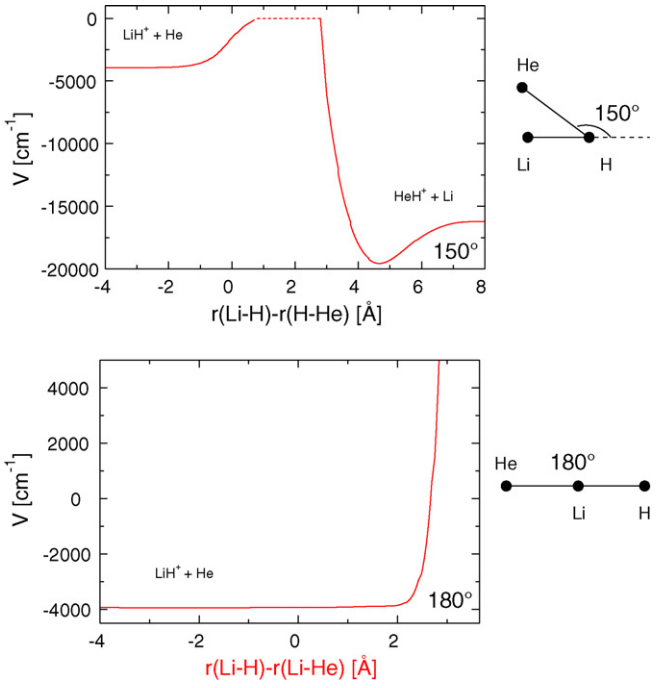

Fig. 6. Same as Fig. 5 at two other orientations. Upper panel: $\theta = 150°$; lower panel: $\theta = 180°$. The dashes in the top panel describe a path around a much higher repulsive region which is not represented here.

cussed before, the first excited surface is isotropic on the side of the charged atom (which is now H^+), although less extended in terms of the range of angles.

When going to angles larger than $\sim 90^\circ$ the approaching helium sees first the repulsive Li atom which constitutes now a barrier to the reaction. At these orientations, once the barrier is overcome, the surface presents however even deeper minima than in the collinear case. This is shown by Fig. 6, upper panel, for an angle of 150° where the well region in the product valley is even more prominent. At 180° (same figure, lower panel), the Li atom represents now a very large barrier, with no possible attachment of He to the H^+ for this conformation as opposed to the small van der Waals minimum observed on the lower surface when the He was approaching the H-side of Li^+H (Fig. 4).

Because of what happened at the angles slightly below this collinear conformation, we further computed the value of the potential fit for an Li–He–H collinear arrangement, and found the global minimum of this surface to be slightly below $-19,000\,cm^{-1}$ for $r_{LiHe} \simeq 4.8$ Å and $r_{HeH} \simeq 0.85$ Å. This fact could not be predicted from only the two extreme collinear approaches described before. The presence of this minimum in this special conformation could be understood in terms of effects from 2B and 3B potentials: the 3B potential is here attractive, while both the strongly bound LiH^+ and HeH^+ cations are near their equilibrium values and the LiHe repulsion amounts to only a few hundred cm^{-1}. Hence, the "insertion" configuration becomes a stable option for this system.

As already discussed for the electronic ground state potential features, two different situations for excited $(LiH^+)^*$ in a helium droplet might be considered to occur. If we take first the interaction of a single $LiH^+(A^2\Sigma^+)$ within the droplet, the exothermicity and absence of barrier of the reaction could make it react very rapidly with the surrounding atoms. This should not depend too much on the initial vibrational energy content of the cation since we have seen that only within a restricted angular region of the PES the LiHe repulsion creates a barrier to the reaction. In fact, to have an initially vibrationally excited $(LiH^+)^*$ should cause an enlargement of the interaction volume spanned by the reactive pathways and hence an even quicker reaction. In any case, the vibrational energy content is relatively small compared to the more than $12,000\,cm^{-1}$ released by the reaction. This energy, when dissipated within the helium droplet may cause its rapid evaporative breakup. If we estimate the binding energy of each He atom in the droplet to be of $\simeq 5\,cm^{-1}$ [25], we find that the droplet has to be made of at least some 2500 atoms in order to release by evaporation all the energy produced by this reaction and still survive as a droplet. Of course, even more helium atoms are required if the LiH^+ is vibrationally excited or if there is more than one LiH^+ entering the droplet.

The presence of a stable "insertion" Li–He–H configuration makes us also wonder as to whether this conformation could be formed inside the droplet. In the solvation process the He atoms usually localise at distances comparable, or larger than, that of the embedded species. Hence, it does not seem probable that one of the He adatoms could manage to overcome the repulsive barrier on the Li-side in order to get stabilised into this conformation.

When discussing the features of the ground state reaction, we saw that the location of the charge on the Li atom led to the formation of a microsolvation cup on the Li-side, while the H atom remained always outside it, at least in the smaller clusters with up to 30 adatoms. For the excited electronic surface the situation becomes different: the charge is being located essentially on the H atom and therefore we expect that it would be this part of the dimer which will be solvated. In case the reaction were to occur very rapidly since a wide range of angular approaches leads to reaction, this will have several consequences, all of which could possibly be detected experimentally: (i) the neutral Li atom could be ejected from the droplet due to its being heliophobic [26]. Such a phenomenon might not be easy to detect because it involves only one particle per event and therefore it will depend on the number of initial dopants in the droplet; (ii) the energy released by the reaction causes a dramatic increase in the number of helium atoms evaporated from the droplet. As mentioned for the case of the ground state processes, this could be detected by He yield measurement or mass spectra, and (iii) the HeH^+ cation could be now formed and it should migrate inside the droplet. Again a laser probe able to scan frequencies close to those of the vibrational ladder of this cation might inform us about its presence and possibly the formation of a snowball surrounding it.

The second process which we could mention here, experimentally in alternative to the direct interaction of an externally prepared LiH^+ species made to enter the droplet, is to activate ionisation inside the droplet. The ionisation process could then be made via charge-exchange with a primary ionised He^+ adatom, although it would also imply the possible involvement of higher electronic states not considered here, or through direct electron or photon impact, where the latter process could also be accompanied with an internal excitation of the formed cationic species Li^+H, a vibrational or even an electronic excitation.

If the excitation is only vibrational, the reaction described in Section 3 for the ground electronic state could also happen before the cation has had time to migrate. In case of the occurrence of the electronic excitation, the symmetries involved allow for dipole emissions: such a process was studied experimentally for alkali dimers [27]. The difference here is that while their reaction implies at most a few thousand cm^{-1} energy release, in our case there are more than $60,000\,cm^{-1}$, which in terms of evaporating He atoms would amount to roughly 15,000 adatoms. Hence this deexcitation process is likely to cause the full destruction of most droplets of that size. This would be even more likely when clusters of dopants are taken in by a droplet.

5. Present conclusions

In the present work we have computed with *ab initio* methods the first two electronic potential energy surfaces for the $[LiHHe]^+$ system. These calculations provide the first fully three-dimensional study on this system. The six diatomic asymptotes (four bound and two not-bound) were successfully fitted, with the vibrational spectrum of the bound diatomics obtained from this fitting in excellent agreement with the data found in the literature. After having fitted the 3B contributions for both the ground and the first excited state we could finally build two global descriptions for these two surfaces.

The important element brought out by the present analysis is the reliable knowledge of the orientational anisotropy existing for both surfaces. The topology of the excited state appears richer, with 3B contributions making insertion configurations with He in between Li and H being significantly (around $2000\,cm^{-1}$) more attractive than the outer collinear conformations.

We also used the two computed surfaces to surmise possible outcomes of the LiH^+ dimer interacting with a helium droplet environment. From the structural point of view, we saw for the ground state that to include the non-rigidity of the cation in the present study could possibly modify the selective collocation of the He adatoms which surround the cationic dopant. On the excited state we found that a barrierless reaction forming HeH^+ could be very likely to occur just after the cation enters in contact with the droplet. We analysed for each deexcitation and/or reactive process predicted by our computed PESs what consequences it would have in terms of He atoms evaporation and cluster restructuring, and how they could be detected in some special instances.

Future work that we are planning on the present system will include the reactive dynamics on both surfaces, the use of diffusion Monte Carlo (DMC) [13] methods to reveal the structures of helium clustering around the ground state cation as a function of its vibrational energy content, and the analysis of what might happen to the excited state of the cation in a droplet. The present calculations will also allow us to extend our current comparative study of LiH^+, LiH and LiH^- interacting with helium, done to see the influence of the charge on the heliophilic/phobic character of the dimer or its mobility inside the droplets, to the analysis of structural effects induced by HeH^+ and $LiHe^+$ formation.

Acknowledgments

M.W. thanks the University of Rome "La Sapienza" for the award of a post-doctoral research fellowship. The Italian Supercomputing Consortium CASPUR is also thanked for providing computational facilities. E.S. thank the FIRB 2005 research programme for the award of a fellowship during the initial stages of the present work.

References

[1] E. Bodo, F.A. Gianturco, R. Martinazzo, Phys. Rep. 384 (2003) 85.
[2] J.P. Toennies, A.F. Vilesov, Ann. Rev. Phys. Chem. 49 (1998) 1.
[3] J.P. Toennies, A.F. Vilesov, Angew. Chem. Int. Ed. 43 (2004) 2622.
[4] F. Stienkemeier, K.K. Lehmann, J. Phys. B 39 (2006) R127.
[5] Y. Ren, V.V. Kresin, Phys. Rev. A 76 (2007).
[6] E. Coccia, E. Bodo, F. Marinetti, F.A. Gianturco, E. Yildrim, M. Yurtsever, E. Yurtsever, J. Chem. Phys. 126 (2007) 124319.
[7] K.P. Atkins, Phys. Rev. 116 (1959) 1339.
[8] M.W. Cole, F. Toigo, Phys. Rev. B 17 (1978) 2054.
[9] J. Kuepper, J.M. Merritt, Int. Rev. Phys. Chem. 26 (2007) 249.
[10] W.K. Lewis, C.M. Lindsay, R.J. Bemish, R.E. Miller, J. Am. Chem. Soc. 127 (2005) 7235.
[11] E. Bodo, F. Sebastianelli, F.A. Gianturco, I. Pino, J. Phys. Chem. A 109 (2005) 4252.
[12] E. Scifoni, E. Bodo, F.A. Gianturco, J. Chem. Phys. 122 (2005) 224312.
[13] C. Di Paola, E. Bodo, F.A. Gianturco, Eur. Phys. J. D 40 (2006) 377.
[14] M.W. Schmidt, K.K. Baldridge, J.A. Boatz, S.T. Ebert, M.S. Gordon, J.H. Jensen, S. Koseki, N. Matsunaga, K.A. Nguyen, S.J. Su, T.L. Windus, M. Dupuis, J.A. Montgomery Jr., J. Comp. Chem. 14 (1993) 1347.
[15] A. Aguado, M. Paniagua, J. Chem. Phys. 96 (1992) 1265.
[16] R.J. LeRoy, LEVEL Programme, U. W. Chem. Phys. Rep. (2007).
[17] S. Bubin, L. Adamowicz, J. Chem. Phys. 125 (2006) 064309.
[18] H. Berriche, F.X. Gadea, Chem. Phys. 203 (1996) 373.
[19] M. Stanke, D. Kedziera, M. Molski, S. Bubin, M. Barysz, L. Adamowicz, Phys. Rev. Lett. 96 (2006) 233002.
[20] A. Slenczka, J.P. Toennies, in: I. Smith (Ed.), Low Temperatures and Cold Molecules. World Scientific, Singapore.
[21] R.A. Guyer, M.D. Miller, Phys. Rev. Lett. 42 (1979) 1754.
[22] K.E. Kürten, M.L. Ristig, Phys. Rev. B 31 (1985) 1346.
[23] M. Lewerenz, B. Schilling, J.P. Toennies, J. Chem. Phys. 102 (1995) 8191.
[24] M. Fárník, J.P. Toennies, J. Chem. Phys. 122 (2005) 014307.
[25] S. Stringari, J. Treiner, J. Chem. Phys. 87 (1987) 5021.
[26] C. Di Paola, F.A. Gianturco, Eur. Phys. J. D 35 (2005) 513.
[27] J. Higgins, C. Callegari, J. Reho, F. Stienkemeier, W. Ernst, M. Gutowski, G. Scoles, J. Phys. Chem. A 102 (1998) 4952.